INTERNATIONAL JOURNAL FOR NUMERICAL METHODS IN FLUIDS
Int. J. Numer. Meth. Fluids 2007; **53**:1173–1193
Published online 22 September 2006 in Wiley InterScience (www.interscience.wiley.com). DOI: 10.1002/fld.1369

Assessment of adaptive and heuristic time stepping for variably saturated flow

C. M. F. D'Haese,[1,*,†] M. Putti[2,‡], C. Paniconi[3,§] and N. E. C. Verhoest[1,¶]

[1]*Laboratory of Hydrology and Water Management (LHWM), Ghent University, Coupure links 653, B-9000 Ghent, Belgium*
[2]*Dipartimento di Metodi e Modelli Matematici per le Scienze Applicate (DMMMSA), University of Padova, Via Belzoni 7, I-35131 Padova, Italy*
[3]*Institut National de la Recherche Scientifique - Centre Eau, Terre et Environnement (INRS-ETE), Université du Québec, 490 de la Couronne, Québec, Canada G1K 9A9*

SUMMARY

The performance of improved initial estimates and 'heuristic' and 'adaptive' techniques for time step control in the iterative solution of Richards equation is evaluated. The so-called heuristic technique uses the convergence behaviour of the iterative scheme to estimate the next time step whereas the adaptive technique regulates the time step on the basis of an approximation of the local time truncation error. The sample problems used to assess these various schemes are characterized by nonuniform (in time) boundary conditions, sharp gradients in the infiltration fronts, and discontinuous derivatives in the soil hydraulic properties. It is found that higher order initial solution estimates improve the convergence of the iterative scheme for both the heuristic and adaptive techniques, with greater overall performance gains for the heuristic scheme, as could be expected. It is also found that the heuristic technique outperforms the adaptive method under strongly nonlinear conditions. Previously reported observations suggesting that adaptive techniques perform best when accuracy requirements on the numerical solution are very stringent are confirmed. Overall both heuristic and adaptive techniques have their limitations, and a more general or mixed time stepping strategy combining truncation error and convergence criteria is recommended for complex problems. Copyright © 2006 John Wiley & Sons, Ltd.

Received 14 February 2006; Revised 10 August 2006; Accepted 11 August 2006

KEY WORDS: numerical modelling; subsurface hydrology; unsaturated zone; Richards' equation; nonlinear processes; adaptive time stepping; time truncation error

*Correspondence to: C. M. F. D'Haese, Laboratory of Hydrology and Water Management (LHWM), Ghent University, Coupure links 653, B-9000 Ghent, Belgium.
†E-mail: Christophe.DHaese@UGent.be
‡E-mail: putti@dmsa.unipd.it
§E-mail: claudio.paniconi@ete.inrs.ca
¶E-mail: niko.verhoest@ugent.be

1. INTRODUCTION

In the numerical modelling of variably saturated flow it is important to combine accuracy with reasonable computing time. The nonlinear character of the governing Richards equation normally requires the use of iterative schemes, such as the Picard method, and efficient simulations can be obtained only if time step adaptation is incorporated into the numerical code. Time step size can be controlled by imposing restrictions on the size of the local time truncation error or by looking at the convergence behaviour of the nonlinear iteration. The first type of approach has been proposed for Richards' equation by Gresho *et al.* [1], Tocci *et al.* [2], Diersch and Perrochet [3], and others. The high order (up to fifth) time integration schemes used in Tocci *et al.* [2] however become competitive against low order schemes such as backward Euler or Crank–Nicolson only when very small relative errors are sought, a case that seldom applies in practical hydrological simulations. Recently, a simpler approach for time step adaptation using low order schemes has been proposed by Kavetski *et al.* [4, 5]. The second, more traditional approach to dynamic time step control is simply, or more heuristically, based on the convergence behaviour of the nonlinear iteration scheme [6]. In this paper we conduct a comparative analysis of the two approaches for a one-dimensional infiltration problem with time-varying boundary conditions [7]. A second infiltration test problem is used to assess the influence of some of the empirical parameters used in the truncation error-based adaptive time stepping scheme.

As will be shown the truncation error-based approach provides successive estimates for the current time step size based on local time truncation errors [4, 5]. In this sense we can consider it to be an *a priori* method, in contrast to the convergence-based approach which provides an estimate for the next time step size and can thus be considered an *a posteriori* method. There is some overlap in these definitions, since in the *a priori* method when the error thresholds or tolerances (global accuracy levels) are met, the solution is accepted and the truncation error estimates are used to calculate the next size, while in the *a posteriori* method when convergence fails the current time step is repeated using successively smaller step sizes. Both approaches provide mechanisms for adapting the time step size in a dynamic manner, but since the terms 'adaptive' and 'heuristic' have been used in the literature to distinguish, respectively, the truncation error-based and convergence-based methods, we will use this convention as well. For brevity and following previous work we will also use abbreviations for adaptive time stepping (ATS) and heuristic time stepping (HTS).

In a linearization scheme such as Picard, the number of iterations needed to converge is a determining factor in the simulation efficiency. One way to enhance the convergence rate of the Picard scheme is to provide the solver with an initial estimate that is closer to the final solution for the current step. Cooley [8] described an extrapolation method for problems involving flow to a well, and this method was also used by Huyakorn *et al.* [9]. In this paper an extrapolation scheme with varying order will be derived and the effects of these improved initial guesses for the Picard scheme will also be evaluated.

Although the functions commonly used to describe soil hydraulic properties are continuous over the entire range of pressure heads, their behaviour, especially near saturation, is such that the derivatives of these functions can exhibit sharp changes (and thus discontinuities in higher order derivatives). Convergence difficulties when using analytical differentiation have been reported, and the use of chord slope methods or other difference approximations has been recommended, either over the entire pressure head range or in a localized fashion (i.e. only for those nodes whose pressure head values are near saturation) [6, 9–11]. This aspect will also be briefly addressed in the paper.

DOI: 10.1002/fld

2. DESCRIPTION OF TIME STEPPING AND EXTRAPOLATION METHODS

Richards' equation can be written using the pressure head (ψ) formulation as

$$\sigma(S_w)\frac{\partial\psi}{\partial t} = \nabla\cdot[K_s K_{rw}(S_w)(\nabla\psi + \eta_z)] + q_s(h) \tag{1}$$

where $\sigma(S_w) = S_w S_s + \phi\partial S_w/\partial\psi$, $S_w(\psi) = \theta(\psi)/\phi$ is water saturation, θ is volumetric moisture content, ϕ is porosity, S_s is the aquifer specific storage coefficient, t is time, ∇ is the gradient operator, K_s is the saturated hydraulic conductivity tensor, $K_{rw}(S_w)$ is the relative hydraulic conductivity function, $\eta_z = (0, 0, 1)^T$, z is the vertical coordinate directed upward, and q_s represents distributed source or sink terms (volumetric flow rate per unit volume). Specification of the nonlinear $S_w(\psi)$ and $K_{rw}(S_w)$ functional relationships, or soil characteristic curves, and of Neumann or Dirichlet boundary conditions, completes the formulation. The van Genuchten and Nielsen [12] expressions for $S_w(\psi)$ and $K_{rw}(S_w)$ are used in this study.

Equation (1) is discretized by linear finite elements in space and a first-order backward Euler scheme in time. This yields the following system of nonlinear algebraic equations:

$$f(\psi^{n+1}) = \left(\frac{C(\psi^{n+1})}{\Delta t^n} + K(\psi^{n+1})\right)\psi^{n+1} - \left(\frac{C(\psi^{n+1})}{\Delta t^n}\right)\psi^n - q(\psi^{n+1}) = 0 \tag{2}$$

where vector ψ^{n+1} contains the nodal pressure head values calculated at time value t^{n+1}, Δt is the time step size, and matrices C and K are the stiffness and mass matrices, respectively. Note that both the stiffness and mass matrices, as well as the source vector, are functions of ψ^{n+1}.

The Picard scheme, also known as successive approximation, is used to solve the nonlinear system (2). In this scheme, the Jacobian matrix is approximated by the system matrix evaluated at the previous nonlinear iteration j, so that the linearized equation becomes [13]

$$J(\psi^{n+1,j})s^{j+1} = -f(\psi^{n+1,j}) \tag{3}$$

where $J = C/\Delta t + K$ and $s^{j+1} = \psi^{n+1,j+1} - \psi^{n+1,j}$. The iteration is repeated until convergence is achieved, i.e. until the norm of s^{j+1} becomes smaller than a preset tolerance.

The initial solution estimate in the iterative procedure is usually the pressure head calculated at the previous time step, i.e. for $j = 0$ we set $\psi^{n+1,0} = \psi^n$. Intuitively, faster convergence is to be expected when the initial solution estimate is as close as possible to the final solution. Thus we see how time step size plays an important role in the convergence behaviour of the iterative scheme; a small Δt means a short step in the transient flow phase which corresponds to small variations in pressure heads. An example where we may obtain unpredictably large or small pressure head changes over the course of a simulation is when time-varying atmospheric forcing is applied as a surface boundary condition. It can be appreciated how dynamic time step adaptation is critical in such cases, since large time steps may be acceptable during certain periods (long interstorm periods with low and constant evaporation, for example) whereas at other times (intense rainfall bursts, for instance) the time step sizes will need to be very small. Note that time step control in these cases should be based on the nonlinear characteristics of the problem instead of estimates of time truncation errors. When a full Newton Jacobian is used, quadratic convergence is expected. In these cases there is in general no restriction on time step size and time step control based on truncation error estimates is optimal [2, 3, 14]. However, quadratic Newton convergence is ensured

DOI: 10.1002/fld

for all cases only in combination with perturbed problems, such as smoothing of characteristic curves and high order time stepping schemes [2, 3, 14, 15]. When using a Picard approach, time step restrictions are introduced by the linearization scheme, and control must be based on the nonlinear behaviour.

2.1. Heuristic time stepping

In HTS, time step control is achieved by looking at the number of iterations needed to achieve convergence, which is an approximate measure of the nonlinearity of the problem. For this reason, and since there is no generally applicable method for predicting the number of iterations to convergence, even though the theoretical rates of convergence for commonly used iterative solvers is known, in practice an *a posteriori* heuristic control is used, as follows. At the end of each time step the step size for the next time level is increased by a factor Δt_{mag} (bounded by a maximum size of $\Delta t_{\max}$) if convergence at the previous time step was achieved in fewer than maxit_1 iterations, it is left unchanged if convergence required between maxit_1 and maxit_2 iterations, and it is decreased by a factor Δt_{red} (bounded by a minimum size of $\Delta t_{\min}$) if convergence required more than maxit_2 iterations. If convergence is not achieved (maximum number of iterations maxit exceeded), the time step is repeated ('back-stepping') using a reduced time step size (factor Δt_{red}, to a minimum of $\Delta t_{\min}$). The values of the three maxit levels and the Δt bounds and multiplicative factors are chosen empirically and are held fixed for the entire simulation.

2.2. Adaptive time stepping

Recently, several adaptive time stepping techniques have been proposed that modify the time step size automatically during a simulation based on local error control, a feature that is not used in heuristic approaches [2, 3, 16]. The adaptive predictor–corrector one-step Newton (PCOSN) scheme by Diersch and Perrochet [3] controls the local time truncation error depending on the predicted and calculated solution for a certain time step. The time step adaptation scheme from this method was originally introduced by Gresho *et al.* [1]. Tocci *et al.* [2] employed the DASPK algorithm which is a variable-step size, variable-order (up to fifth-order) differential algebraic equation (DAE) solver on the pressure head based form of Richards' equation. In this approach, estimates of temporal truncation error were used explicitly to control the solution order, which ranged from first- to fifth-order in time, and the time step size. Their work points out that adaptive time stepping becomes comparatively efficient only when using higher order DASPK or when higher accuracy levels are required. Fixed time step methods, as well as many cases of simple adaptive time stepping methods, provided better performance than a first-order restricted version of DASPK. Williams and Miller [16] used a method to solve a transformed version of Richards' equation in combination with a variable-order, variable-step size solver. They concluded that this solver is more effective than heuristic time stepping for intermediate to high levels of accuracy.

In our finite element model overall accuracy is limited by the Euler time discretization scheme used. The ATS method proposed by Kavetski *et al.* [4, 5] is applicable to this scheme and is quite straightforward to implement in existing software. The ATS approach evaluates the local time truncation error by calculating the difference between solutions of different accuracy. To this aim, ψ^{n+1} in (2) can be thought of as the result of a first-order Taylor series expansion

$$\psi_1^{n+1} \approx \psi^n + \Delta t^n \dot{\psi}^{n+1} \tag{4}$$

DOI: 10.1002/fld

where $\dot{\psi}$ indicates time derivative. The accuracy of this approximation can be raised to second-order by averaging the derivative estimates from consecutive time levels [4]

$$\psi_2^{n+1} \approx \psi^n + \tfrac{1}{2}\Delta t^n (\dot{\psi}^n + \dot{\psi}^{n+1}) \tag{5}$$

The difference between these first- and second-order approximations is an $O(\Delta t^2)$ approximation of the truncation error incurred during the $(n+1)$th time step from $t^n \to t^{n+1}$ with time step size Δt^n [5]

$$e^{n+1} \approx |\psi_1^{n+1} - \psi_2^{n+1}| = 1/2\Delta t^n |\dot{\psi}^{n+1} - \dot{\psi}^n| \approx 1/2(\Delta t^n)^2 |\ddot{\psi}^n| \tag{6}$$

where we have used the L2 norm in evaluating this expression. The approach suggested by Kavetski *et al.* [4] substitutes (4) into (2) and solves for $\dot{\psi}$. In our implementation we solve for ψ and evaluate $\dot{\psi}$ by finite differences using the pressure heads calculated at previous times, as suggested by Kavetski *et al.* [4, 5, 10].

Although the infinity norm $\|e\|_\infty$ can be used to constrain the largest absolute error across the entire soil pressure profile, it is preferable, especially in the case of flow in both saturated and unsaturated media, to use a mixed absolute-relative error criterion, i.e. the time step is accepted if

$$\max_i (e_i^{n+1} - \tau_R |\psi_i^{n+1}| - \tau_A) < 0 \tag{7}$$

where τ_A and τ_R are absolute and relative error tolerances, respectively, and i indexes the nodes in the spatial mesh. The node index with the largest error measure is stored as iCrit to be used in the step size selectors described below. It can be observed that as $|\psi| \to 0$, the absolute error criterion dominates, whereas if $|\psi|$ is large the relative error component will be decisive.

If the error criterion (7) is met, the size Δt_1^{n+1} of the next time step is calculated as

$$\Delta t_1^{n+1} = \Delta t^n \times \min\left(s \sqrt{\frac{\tau_R |\psi_{i\text{Crit}}^{n+1}| + \tau_A}{\max(e_{i\text{Crit}}^{n+1}, \text{EPS})}}, r_{\max} \right) \tag{8}$$

If the error criterion is not satisfied, a back-stepping mechanism is activated whereby the current time step is repeated as many times as needed using a reduced step size, calculated with successive values $e_{i\text{Crit},k}$ rather than $e_{i\text{Crit}}$

$$\Delta t_{k+1}^n = \Delta t_k^n \times \max\left(s \sqrt{\frac{\tau_R |\psi_{i\text{Crit},k}^{n+1}| + \tau_A}{\max(e_{i\text{Crit},k}^{n+1}, \text{EPS})}}, r_{\min} \right) \tag{9}$$

where the subscript k indexes consecutive step size estimates. When this occurs, we refer to the k (>1) back-steps as 'failed steps', to distinguish them from the back-steps that occur when the iterative solver does not converge (which can happen for both the ATS and HTS schemes). When the latter happens in ATS, there is not sufficient information for calculating a reduced time step size with (9) and so HTS-type time step reduction is used. We refer to these occurrences (for both HTS and ATS) as 'back-steps' in the test case results.

A number of empirical parameters are used to increase the robustness of the estimates in (8) and (9): $r_{\max}$ and $r_{\min}$ limit the multiplication and reduction factors and are often set equal to 4.0 and 0.1, respectively; s is a safety factor ($s \sim 0.8$–0.9); EPS is a machine zero approximation (usually set to 10^{-10}) that guards against floating point errors [5].

DOI: 10.1002/fld

2.3. Initial solution estimates

Extrapolation can be used to improve the initial solution estimate for Picard iteration. In Cooley [8] and Huyakorn *et al.* [9] a first-order extrapolation method is described. We implement instead a second-order extrapolation method, similar to a scheme presented by Diersch and Perrochet [3], that is derived as follows. This scheme differs from the one used in References [4, 5] by taking into account all the second-order terms in the Taylor expansion. The Taylor expansion of ψ^{n+1} around ψ^n is

$$\psi^{n+1} = \psi^n + \Delta t^n \dot{\psi}^n + \frac{(\Delta t^n)^2}{2!}\ddot{\psi}^n + \cdots \tag{10}$$

Approximating $\dot{\psi}$ and $\ddot{\psi}$ by Taylor series using ψ^n, ψ^{n-1}, and ψ^{n-2} we obtain

$$\psi^{n+1} \approx \psi^n + \Delta t^n \left(\frac{\psi^n - \psi^{n-1}}{\Delta t^{n-1}} \right) + \frac{1}{2}\left(\frac{(\Delta t^n)^2}{\Delta t^{n-1}} + \Delta t^n \right) \cdot \left(\frac{\psi^n - \psi^{n-1}}{\Delta t^{n-1}} - \frac{\psi^{n-1} - \psi^{n-2}}{\Delta t^{n-2}} \right) \tag{11}$$

This equation can be used to improve the initial estimate for the nonlinear iterative solver at the beginning of each time step. Taking only the first term into account results in the standard, zeroth-order, procedure of setting $\psi^{n+1,0} = \psi^n$, including the second term gives a first-order estimate, and taking all three terms into account gives a second-order extrapolation.

2.4. Chord slope evaluation of the characteristic curves

The soil characteristic curves $S_w(\psi) = \theta(\psi)/\phi$ and $K_{rw}(S_w)$ used in the test cases are given by van Genuchten and Nielsen [12]

$$\begin{aligned} \theta(\psi) &= \frac{\theta_s - \theta_r}{[1 + (\alpha|\psi|)^n]^m} + \theta_r, \quad \psi \leqslant 0 \\ \theta(\psi) &= \theta_s, \qquad \psi > 0 \end{aligned} \tag{12}$$

$$\begin{aligned} K(\psi) &= K_s K_{rw}(\psi) = K_s(1 - (\alpha|\psi|)^{n-1}[1 + (\alpha|\psi|)^n]^{-m})^2/[1 + (\alpha|\psi|)^n]^{m/2}, \quad \psi \leqslant 0 \\ K(\psi) &= K_s, \qquad \psi > 0 \end{aligned} \tag{13}$$

where θ_r is the residual moisture content, θ_s ($= \phi$) is the saturated moisture content, $m = 1 - 1/n$, and n and α are fitting parameters. Equation (1) contains the derivative of the water saturation S_w, or equivalently moisture content θ, with respect to pressure head, given as

$$\begin{aligned} \frac{d\theta}{d\psi} &= \frac{(n-1)(\theta_r - \theta_s)|\psi|^{n-1}}{\alpha^{-n}[1 + (\alpha|\psi|)^n]^{m+1}}, \quad \psi \leqslant 0 \\ \frac{d\theta}{d\psi} &= 0, \qquad \psi > 0 \end{aligned} \tag{14}$$

DOI: 10.1002/fld

In some of the simulations we ran severe difficulties were encountered when this analytical expression for the derivative was used. This may be due to the shape of the water capacity function $\partial\theta/\partial\psi$ and the relative conductivity function $K_r(\psi)$ near saturation [15]. For instance, the slopes change from $-\infty$ for $\partial\theta/\partial\psi$ and ∞ for $K_r(\psi)$ when $n<2$ to zero when $n>2$. In order to attempt to overcome this problem, two variants of a chord slope technique combined with a centred difference formula were used [9, 11]. One variant uses the pressure head at the previous time step, the other at the previous nonlinear iteration. If the absolute difference between the pressure head at the current nonlinear iteration and the pressure head at the previous time step (or previous nonlinear iteration), i.e. $|\psi^{n+1,j+1} - \psi^n|$ ($|\psi^{n+1,j+1} - \psi^{n+1,j}|$) is smaller than a user specified tolerance TOLKSL (0.005 m was used in the test problems), the centred difference formula is used

$$\frac{d\theta}{d\psi} = \frac{\theta(\psi + \text{TOLKSL}) - \theta(\psi - \text{TOLKSL})}{2\text{TOLKSL}} \tag{15}$$

If this absolute difference is larger than TOLKSL, a chord slope approximation is used

$$\frac{d\theta}{d\psi} = \frac{\theta(\psi^{n+1,j+1}) - \theta(\psi^n)}{\psi^{n+1,j+1} - \psi^n} \quad \text{or} \quad \frac{d\theta}{d\psi} = \frac{\theta(\psi^{n+1,j+1}) - \theta(\psi^{n+1,j})}{\psi^{n+1,j+1} - \psi^{n+1,j}} \tag{16}$$

3. NUMERICAL TESTS

3.1. Test problem 1

Comparison between HTS and ATS is performed on the test case proposed by Kavetski *et al.* [10]. The problem considers a soil column of 2.0 m length discretized with a vertical resolution $\Delta z = 0.00625$ m. The bottom of the column is a water table boundary condition (i.e. $\psi = 0$) while a time-dependent Dirichlet condition is imposed at the top boundary (Figure 1)

$$\psi(z=2, t) = \begin{cases} -0.05 + 0.03\sin(2\pi t/100\,000), & \text{T1:} \quad 0 < t \leqslant 100\,000 \text{ s} \\ 0.1, & \text{T2:} \quad 100\,000 < t \leqslant 180\,000 \text{ s} \\ -0.05 + 2952.45\exp(-t/18\,204.8), & \text{T3:} \quad 180\,000 < t \leqslant 300\,000 \text{ s} \end{cases} \tag{17}$$

The initial pressure head distribution is

$$\psi(z, t=0) = \begin{cases} -0.05 + \dfrac{0.05 - 1.99375}{0.00625}(z-2), & 1.99375 \leqslant z \leqslant 2 \\ -z, & 0 \leqslant z < 1.99375 \end{cases} \tag{18}$$

The soil parameters are $\theta_r = 0.095$, $\phi = 0.410$, $\alpha = 1.9\,\text{m}^{-1}$, $n = 1.31$, $K_s = 0.062$ m/d, and soil elastic storage $S_s = 0.41 \times 10^{-4}\,\text{m}^{-1}$. These soil properties correspond to an unconsolidated clay loam with a nonuniform grain size distribution [14]. Kavetski *et al.* [5] carried out a similar comparison using a moisture-based form of Richards' equation and a different test case that does not feature a time-varying boundary conditions with surface ponding.

Table I summarizes the results for the first 100 000 s of simulation time (period T1 in Figure 1) for ATS and HTS with zero- and second-order initial solution estimates (ATS-0, ATS-2, HTS-0, HTS-2). The ATS parameters were $\tau_R = 0.0$, $\tau_A = 0.001$, $s = 0.85$, $r_{max} = 4.0$, $r_{min} = 0.1$, and

DOI: 10.1002/fld

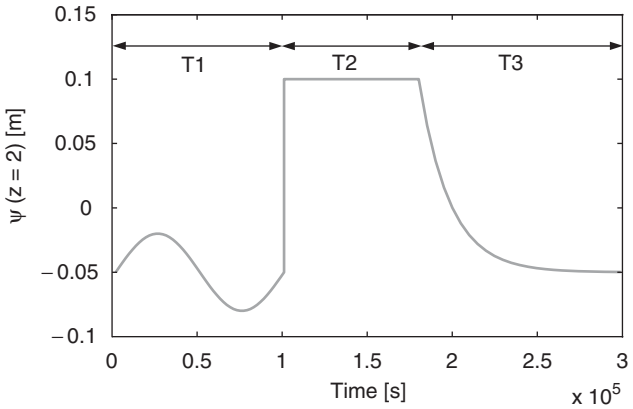

Figure 1. Dirichlet boundary condition imposed at the top of the soil column versus time for the first test problem.

Table I. Comparison of ATS and HTS with zero- and second-order initial solution estimates for the first 100 000 s. CPU times are relative to ATS-2.

Order of initial estimate	Exact solution	ATS 0	ATS 2	HTS 0	HTS 2
CPU time		1.44	1	8.38	1.15
Number of time steps	2134	525	524	4668	635
Nonlinear iterations	8903	3277	2221	18 799	2556
Total cum. abs. MBE (%)	0.29	1.68	1.68	1.00	1.49
MAE (mean absolute error) (m)		8.090×10^{-4}	8.090×10^{-4}	6.284×10^{-4}	3.536×10^{-4}
RMSE (m)		0.0029	0.0029	0.0023	0.0010

$\text{EPS} = 1 \times 10^{-10}$. For HTS we set $\Delta t_{\text{mag}} = 1.1$, $\Delta t_{\text{red}} = 0.8$, $\Delta t_{\text{max}} = 5000$, $\Delta t_{\text{min}} = 1 \times 10^{-6}$, $\text{maxit}_1 = 8$, and $\text{maxit}_2 = 4$. For both the ATS and HTS schemes the maximum number of iterations, maxit, was 50 and the convergence tolerance on the L_2 norm of the error, τ_{PI}, was 10^{-6}. The initial time step size Δt^0 was 10 s. Derivatives of the moisture characteristics were calculated analytically. A surrogate exact solution for this T1 period is evaluated numberically using the HTS scheme with an iteration error tolerance $= 10^{-8}$ ($\Delta t_{\text{red}} = 0.67$ and $\Delta t_{\text{mag}} = 1.5$) and a vertical resolution $\Delta z = 0.001$ m. The accuracy for each of the ATS and HTS simulations is evaluated by means of the mean absolute error (MAE) and root mean square error (RMSE) calculated with respect to the surrogate exact solution. From these statistics in Table I it can be concluded that all runs have adequate and comparable accuracy. The results for the ATS implementation are very similar to those obtained by Kavetski *et al.* [10]. There is very little difference between the use of zero- or second-order extrapolation in the total number of time steps, but a significant reduction in nonlinear iterations is obtained for ATS-2. This shows the beneficial effects of an accurate initial guess for the convergence of the Picard technique. HTS shows a much larger difference in performance between the zero- and second-order alternatives. The mass balance errors for the HTS runs are slightly lower than those for the ATS runs. Using second-order extrapolation results

DOI: 10.1002/fld

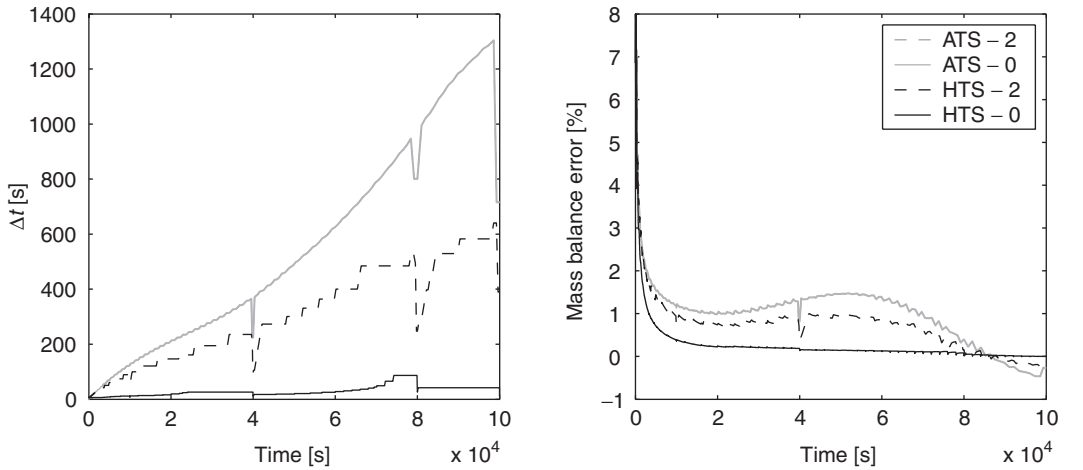

Figure 2. Evolution of Δt and mass balance errors during the first 100 000 s of the test case simulation. ATS-0 and ATS-2 show similar behaviour, while extrapolation order has a great effect on HTS.

in a considerable gain in numerical performance arising from the much larger step sizes that were made possible, as can be seen from Figure 2. Although the number of time steps for HTS-2 is approximately 20% higher than for ATS-2, the number of nonlinear iterations is less than 10% higher. For both ATS-2 and HTS-2 on average about four nonlinear iterations per time step are performed. These results suggest that the nonlinearity in this part (T1) of the simulation is relatively mild and the Picard scheme behaves reasonably well.

The evolution of Δt (Figure 2) is different for ATS and HTS. ATS shows a smooth increase of the step size, which is one of the objectives of the method, with an always larger Δt compared to HTS, causing in turn larger mass balance errors (MBE) compared to HTS. In fact, HTS with zero-order extrapolation, which results in very small step sizes throughout the simulation, yields the smallest MBE. For all four schemes the MBEs are nonetheless acceptably small (at most a few per cent).

Analysis of the first 100 000 s of the test case simulation shows that second-order extrapolated initial guesses are very effective in enhancing the convergence properties of the Picard linearization.

The second period (T2, $100\,000 \leqslant t \leqslant 180\,000$) is very challenging for numerical solvers. Because of the sudden increase of the upper Dirichlet boundary condition to a positive value of 0.1 m (ponding), a sharp moisture front infiltrates into the soil column. At the beginning of the third period (T3) ponding decreases exponentially, reaching asymptotically a final value of -0.05 m, and by the end of the simulation the entire column is close to full saturation (Figure 3). Attempts to simulate the entire period with analytical differentiation of the moisture characteristics resulted in infinitely small time step sizes and endless run times for both the ATS and HTS schemes. For this reason the two chord slope techniques described earlier were used, labeled $\psi^{n+1,j}$ (pressure head at the previous nonlinear iteration) and ψ^n (pressure head at the previous time step). All simulations were calculated using $\Delta t_{\text{red}} = 0.25$.

In Figure 4 we plot the evolution of Δt, MBE, and cumulative MBE. At the end of T1 large time steps are attained, but these drop dramatically in period T2. In this ponding period a slight

DOI: 10.1002/fld

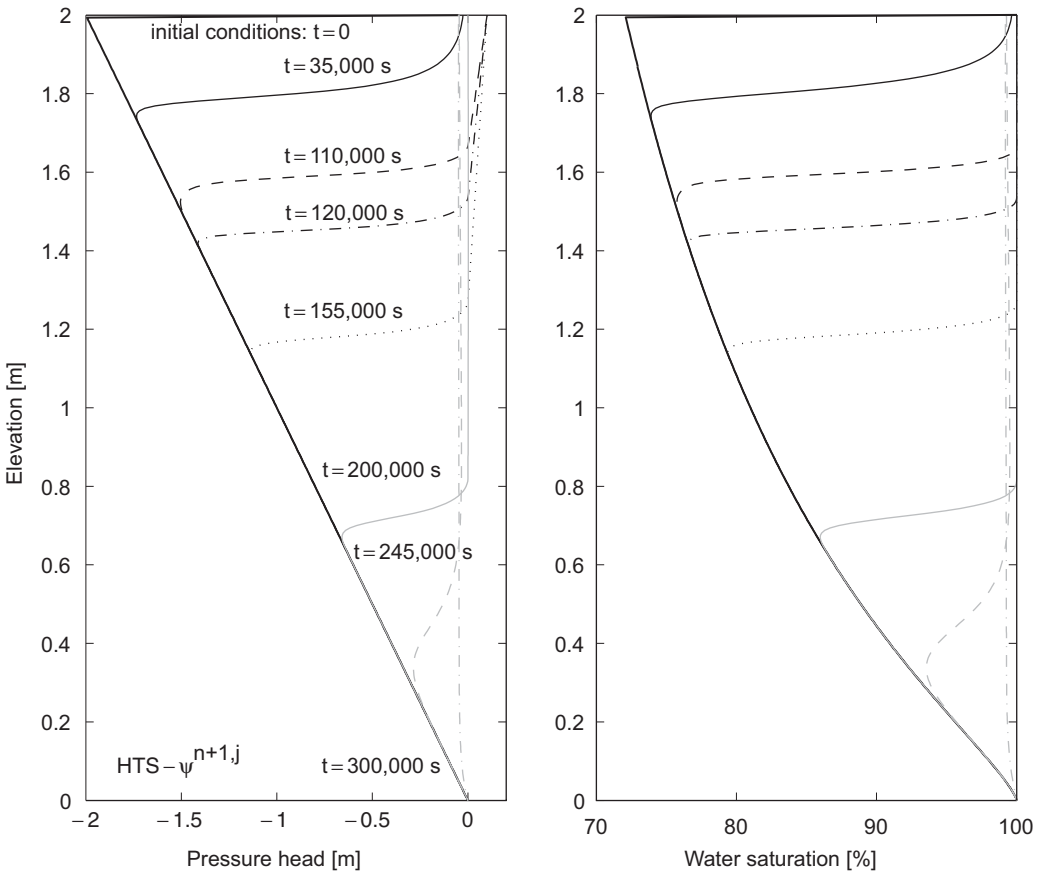

Figure 3. Pressure head (left) and water saturation (right) profiles. The results shown are for HTS with the chord slope technique based on the previous nonlinear iteration. The other schemes produced very similar profiles.

increasing trend in time step size can nevertheless be observed, although strong oscillations also occur. These oscillations have been attributed to insufficient spatial resolution [4, 5]. The time step size remains small from 180 000 to 200 000 s, as ponding gradually decreases to zero. In the final period Δt increases rapidly and reaches large values (up to about 3000 s for ATS). This indicates easier nonlinear solver conditions due to smoother infiltration fronts and surface conditions that are no longer fully saturated.

In the HTS runs, the MBE remains almost constant and close to zero, except for a few time steps around 100 000 s. The peak in mass balance error for all the ATS simulations at the transition from T1 to T2 is caused by the fact that the error control mechanism was switched off in an interval of 40 s centered at $t = 100\,000$ s. This was necessary because even very small time steps were rejected by the ATS error criterion. The reason for this behaviour may be attributed to the fact that the truncation error estimator based on ψ^n does not take into consideration the drastic change in nonlinearities due to the jump in the boundary conditions. This solution is similar to

DOI: 10.1002/fld

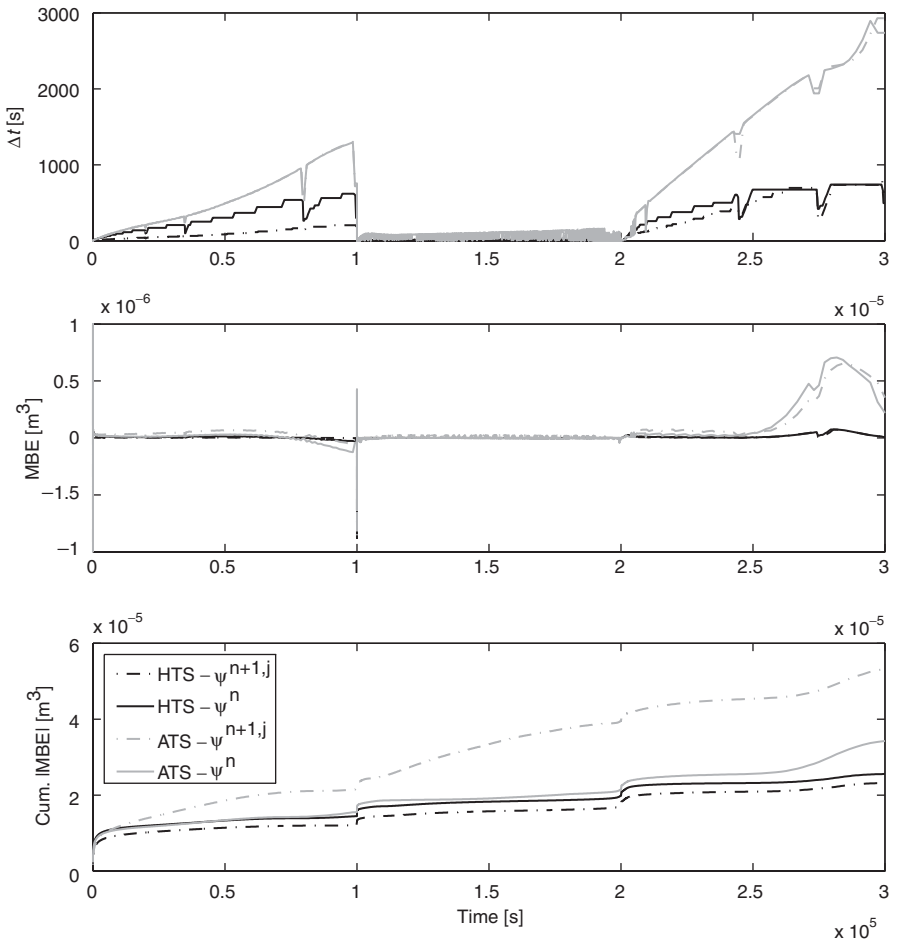

Figure 4. Evolution of Δt and mass balance errors for the entire simulation.

the one proposed by Kavetski *et al.* [5] who used an internal re-initialization in order to overcome problems associated with discontinuous boundary conditions. The ATS runs show an additional MBE peak at about 280 000 s due possibly to too-large time step sizes. Generally, it can be stated that the MBEs are proportional to time step size for both ATS and HTS, in agreement with theory.

Other simulation statistics are summarized in Table II. The mass balance error (MBE) at any given time step is calculated as the absolute difference between the changes in water storage during that time step. The change in water storage is calculated in two ways, as the difference between incoming and outgoing water volumes and from changes in volumetric moisture content caused by differences in pressure head between the current and the previous time level. The total time steps and linear iterations used by the ATS scheme with ψ^n-based chord slope during T1 (522 and 2331, respectively) are comparable to those reported in Kavetski *et al.* [10] (559 and 2153,

DOI: 10.1002/fld

Table II. Comparison of ATS and HTS for the first test problem. CPU times are relative to HTS-ψ^n.

Time stepping technique Chord slope technique:	HTS $\psi^{n+1,j}$	HTS ψ^n	ATS $\psi^{n+1,j}$	ATS ψ^n	ATS-0 ψ^n	Kavetski *et al.* [10]
CPU time	1.01	1	1.30	1.68	2.22	
Total successful time steps	530 975	528 102	61 444	80 108	107 077	368 396
Total nonlinear iterations	2 367 611	2 351 613	3 191 527	4 171 999	5 585 761	
Time steps in T1	2148	647	533	522	523	559
Average Δt in T1 (s)	4.655×10^1	1.546×10^2	1.876×10^2	1.916×10^2	1.912×10^2	1.789×10^2
Nonlinear iterations in T1	8517	2577	2793	2205	3271	
Avg # nonlin it/Δt	3.97	3.98	5.24	4.22	6.25	
Time steps in T2	426 396	425 589	28 490	34 531	42 006	279 707
Average Δt in T2 (s)	1.876×10^{-1}	1.880×10^{-2}	2.808×10^0	2.317×10^0	1.904×10^0	2.860×10^{-1}
Nonlinear iterations in T2	1 894 045	1 885 783	1 469 759	1 788 558	2 179 632	
Avg # nonlin it/Δt	4.44	4.43	51.59	51.80	51.89	
Time steps in T3	102 431	101 866	32 421	45 055	64 548	88 130
Average Δt in T3 (s)	1.172×10^0	1.178×10^0	3.701×10^0	2.663×10^0	1.859×10^0	1.362×10^0
Nonlinear iterations in T3	465 049	463 253	1 718 975	2 381 236	3 402 858	
Avg # nonlin it/Δt	4.54	4.56	53.02	52.85	52.72	
Total failed steps	Not applicable	Not applicable	41	40	46	53
Total back-steps	29 812	29 733	59 789	78 508	105 448	189 814
Total cum. abs. MBE (m^3)	2.318×10^{-5}	2.555×10^{-5}	5.320×10^{-5}	3.424×10^{-5}	3.390×10^{-5}	
Total cum. abs. MBE (%)	0.43	0.47	0.98	0.63	0.63	0.05

DOI: 10.1002/fld

respectively), whereas for the entire period our ATS implementation required 4.6 times fewer steps than in Kavetski *et al.* [10]. HTS requires a much larger number of time steps, but fewer nonlinear iterations, resulting in a 30% save in CPU with respect to ATS. While no significant difference can be seen in the results of the two chord slope approaches for HTS, ATS-$\psi^{n+1,j}$ appears to outperform ATS-ψ^n, in particular for the last two simulation periods. Linear iterations, not reported in Table II, were typically 1–2 per nonlinear iteration for all simulations.

Examining more closely the HTS-ψ^n and ATS-$\psi^{n+1,j}$ schemes, we note that HTS resulted in significantly fewer back-stepping occurrences. The reason for this is that the step sizes predicted by ATS, while ensuring low truncation error, do not guarantee convergence of the Picard scheme. If the nonlinear solver does not converge, the back-stepping mechanism is activated whereby the current time step is repeated with a reduced time step, obtained by multiplying Δt with Δt_{red} $(=0.8)$. This smaller Δt might result in a low truncation error, setting the ATS magnification factor for calculating the next time step size (Equation (8)) almost always equal to its maximum value of $r_{\max}$. Due to this sudden increase in Δt, the Picard scheme will probably again not converge, and the back-stepping mechanism is activated again.

Under highly nonlinear conditions, convergence evidently requires time step sizes that are much smaller than those dictated by accuracy considerations alone. This suggests that time step adaptation based on error control may not be optimal. On the other hand, HTS looks at the nonlinear convergence behaviour and is more conservative in increasing the time step size. A mixed form of time step adaptation may therefore be the best approach, giving more weight to error-based control when nonlinearities are mild, and to nonlinear convergence behaviour otherwise. Indeed effective schemes for solving nonlinear equations necessarily interact with the step size selection strategy. A comprehensive approach should use all the information that can be gathered from the entire simulation (e.g. error estimation, nonlinear behaviour, boundary conditions and forcing function variations). Optimization techniques together with optimal control theory provide in this sense an ideal framework for the solution of this problem, as suggested by Gustafsson and Söderlind [17].

3.1.1. Zoom on first switch in boundary conditions (at 100 000 s). We examine more closely, for the transition period from T1 to T2, the influence of the time step magnification and reduction factors, namely Δt_{mag} for HTS, $r_{\max}$ for ATS, and Δt_{red} for both schemes when Picard iteration does not converge. The values for these parameters are given in Table III, along with the results, which are also shown in Figure 5. Second-order initial solution estimates were used for all runs.

Several points can be highlighted from the results shown in Table III. The best CPU times are obtained for the least aggressive time stepping methods, i.e. those with small values of Δt_{mag} or $r_{\max}$. For ATS this is obtained with the $\psi^{n+1,j}$ chord slope option and for HTS with the ψ^n option. The runs with more aggressive time stepping required CPU resources up to 44 times greater than the less aggressive runs. Although the more aggressive runs required few nonlinear and linear iterations per time step in the first period to 100 000 s (see Tables II and III), it is evident that many more are needed after 100 000 s when ponding sets in. In the first period HTS and ATS produce comparable results. ATS shows a smooth evolution in Δt (Figure 5), the reason being that the nonlinearities are not so large during T1 and the simulation is controlled by the time truncation error. As a consequence, the magnification factors calculated by the ATS scheme (Equation (8)) never attain their maximum value of $r_{\max}$. After switching to ponding, however, the nonlinearity

DOI: 10.1002/fld

Table III. Comparison between ATS and HTS for the time period between 0 and 100 200 s for different time step magnification and reduction factors. CPU times are relative to HTS-ψ^n.

Chord slope technique: time stepping technique Δt_{mag} or $r_{\max}$, Δt_{red}	$\psi^{n+1,j}$ HTS 1.5, 0.67	HTS 4, 0.25	ATS 1.5, 0.67	ATS 4, 0.25	ψ^n HTS 1.5, 0.67	HTS 4, 0.25	ATS 1.5, 0.67	ATS 4, 0.25
CPU time	3.02	44.09	1.82	6.01	1	28.13	9.67	11.96
Time steps in $[0 \rightarrow 100\,000]$ s	1786	1169	530	533	555	417	525	522
Nonlinear iterations in $[0 \rightarrow 100\,000]$ s	7162	4898	2779	2793	2328	1985	2212	2205
Time steps in $[100\,000 \rightarrow 100\,200]$ s	2	2400	72	292	2	1628	473	601
Nonlinear iterations in $[100\,000 \rightarrow 100\,200]$ s	112	106 208	1677	12 209	81	68 686	22 004	27 820
Total failed steps	Not applic.	Not applic.	10	11	Not applic.	Not applic.	15	13
Total back-steps	1	1993	21	214	1	1281	398	514
Total cum. abs. MBE (m^3)	3.58×10^{-5}	2.81×10^{-5}	2.70×10^{-5}	2.50×10^{-5}	2.29×10^{-5}	2.08×10^{-5}	1.72×10^{-5}	1.74×10^{-5}
Total cum. abs. MBE (%)	2.67	2.10	2.00	1.85	1.70	1.54	1.28	1.29

DOI: 10.1002/fld

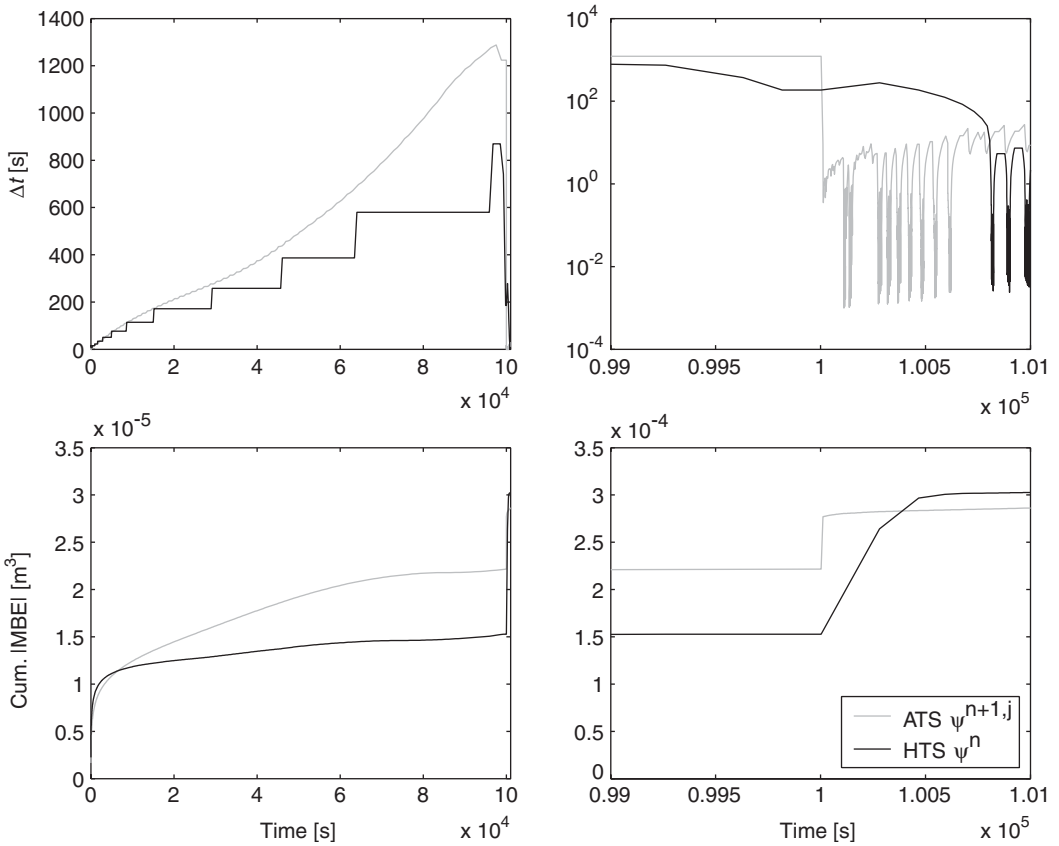

Figure 5. Evolution of Δt and cumulative mass balance error for the time period between 0 and 101 000 s. The plots on the left show the evolution from 0 to 101 000 s while the plots on the right focus on the 2000-second period around the switch in boundary conditions. Note the logarithmic scaling for the zoomed Δt axis.

strongly increases and time step sizes need to be kept very small in order to achieve convergence of the iterative Picard scheme. These small time steps produce very small time truncation errors, resulting in maximal ($\Delta t \times r_{\max}$) time step projections in ATS. The result is a strongly oscillating time step size between the values imposed by convergence requirements and those suggested by truncation error estimates, as can be clearly seen in Figure 5. In Figure 5 we also see that both schemes show a jump in MBE after 100 000 s.

3.2. Test problem 2

In order to evaluate the influence of the different ATS parameters, a vertical infiltration problem in a 60 cm soil column [4, 11, 18] will be solved. This soil column is parameterized using the van Genuchten relationships with $K_s = 9.22 \times 10^{-5}$ m/s, $\theta_r = 0.102$, $\theta_s = 0.368$, $\alpha = 3.350\,\mathrm{m}^{-1}$, and $n = 2$. A vertical discretization of 0.6 cm is used. The Dirichlet boundary conditions are

DOI: 10.1002/fld

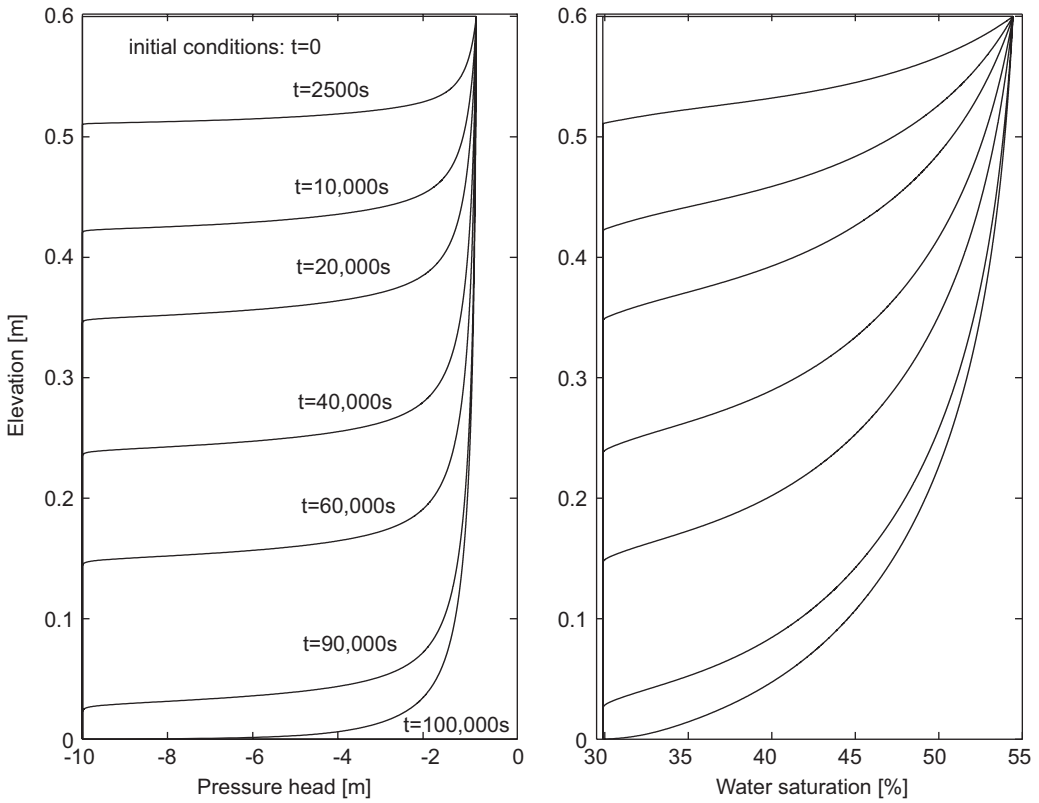

Figure 6. Pressure head (left) and water saturation (right) profiles for the second test problem.

$\psi(z=0.6\,\text{m}, t) = -0.75\,\text{m}$ and $\psi(z=0, t) = -10\,\text{m}$. The initial pressure profile is specified as

$$\begin{aligned}\psi(z, t=0) &= -0.75\,\text{m} \quad z > 0.594\,\text{m} \\ &= -10\,\text{m} \quad z \leqslant 0.594\,\text{m}\end{aligned} \tag{19}$$

These forcing conditions lead to the development of a sharp infiltration front and induce large gradients in the solution. We used analytical differentiation of the soil characteristic curves and second-order initial solution estimates for all runs.

Because it is not possible to obtain an analytical solution for this problem, a surrogate exact solution is evaluated numerically using the ATS scheme with a truncation error tolerance $\tau_R = 10^{-7}$, $\tau_A = 10^{-3}$, and an iteration tolerance $\tau_{PI} = 10^{-9}$ [4]. Although it is not necessary to set $\tau_{PI} < \tau_R$, it may be prudent to do so to ensure that residual nonlinear solver errors do not exceed the local temporal truncation errors. In order to obtain a surrogate exact solution as accurate as possible, consecutive vertical refinements of the grid were made using 100, 1000, and 5000 layers. This resulted in decreasing mass balance errors, with the lowest value of 8.17% obtained for the 5000-layer run. Figure 6 shows the pressure head and the water saturation profiles for this test problem.

DOI: 10.1002/fld

Table IV. Numerical performance for different r_{max} values. CPU times are relative to $r_{max} = 1.5$.

r_{max}	Exact solution	1.5	2	3	4
CPU time		1	1.54	2.50	2.56
Total successful time steps	31 675	1622	1959	2417	2129
Average time step size (s)	3.157×10^1	6.165×10^1	5.105×10^1	4.137×10^1	4.697×10^1
Total nonlinear iterations	177 589	11 472	18 163	28 362	29 877
Total failed steps	6	1011	1901	3251	3177
Total back-steps	15	0	0	0	0
Total cum. abs. MBE (m^3)	1.547×10^{-4}	2.981×10^{-4}	2.946×10^{-4}	2.916×10^{-4}	2.939×10^{-4}
Total cum. abs. MBE (%)	8.17	14.98	14.81	14.67	14.78

We will assess the influence of ATS parameters r_{max}, τ_A, and τ_R. For all runs the other ATS parameters are $s = 0.85$, $r_{min} = 0.1$, EPS $= 10^{-10}$. The initial time step size is 0.1 s.

3.2.1. Influence of r_{max}. The ATS parameter r_{max} in Equation (8) is intended to prevent spuriously large step size changes. Although Kavetski *et al.* [4] suggest to keep this parameter fixed to a value of 4, the influence of this parameter on computational efficiency and accuracy is investigated via several runs using r_{max} values of 1.5, 2, 3, and 4 (Table IV).In these runs we used $\tau_R = 10^{-2}$, $\tau_A = 10^{-3}$, and $\tau_{PI} = 10^{-4}$. Contrary to what one might expect, increasing r_{max} does not necessarily result in a more efficient simulation. When the error criterion (7) is met, a magnification factor is calculated that apparently can be too optimistic or aggressive when not reset by a sufficiently low limiting value of r_{max}. This increases the probability of failed steps in subsequent time steps, as is clear from Table IV, as well as the frequency of MAGFAC values less than 1.0, i.e. reductions in time step size to correct for previous overestimations(Figure 7).

The interesting thing about the fact that better performance is obtained with lower r_{max} values (at least in this test case), while recognizing that lower r_{max} also means that the percentage of time steps for which MAGFAC $= r_{max}$ increases (over 80% for $r_{max} = 1.5$ in Figure 7), is that when MAGFAC $= r_{max}$ the ATS scheme reduces to an essentially 'heuristic' method (more rudimentary even than the HTS scheme since there are no $maxit_1$ and $maxit_2$ thresholds).

Also surprising in Figure 7 is the extremely low frequency of time steps for which ATS actually predicts (without being overridden by r_{max}) an increase in time step size (i.e. $1 <$ MAGFAC $< r_{max}$). One might expect that when the error criterion (7) is met, step size increases would be more prevalent than step size reductions. Indeed this is what we observe for the 'exact' solution. Interestingly the 'exact' solution in Figure 7 is also the only case where MAGFAC $= r_{max}$ hardly ever occurs. Taken together, these two observations seem to suggest that the ATS scheme, as with the DASPK method mentioned earlier, is most effective when the accuracy requirements on the numerical solution are high or stringent.

3.2.2. Influence of τ_A. Three different values of parameter τ_A in the error criterion (7) will be simulated: 0.001, 0.01 and 0.1 m. τ_R is kept constant at 10^{-2} and $\tau_{PI} = 10^{-4}$. For the surrogate exact solution $\tau_A = 0.001$ and $\tau_R = 10^{-7}$.

In Figure 8 we see that the $\tau_A = 0.1$ simulation is noticeably less accurate than the others, with pressure head errors as large as 2 m. This is also seen in Figure 9, where the larger time step sizes enabled by a low accuracy requirement also produce, as expected, higher mass balance errors.

DOI: 10.1002/fld

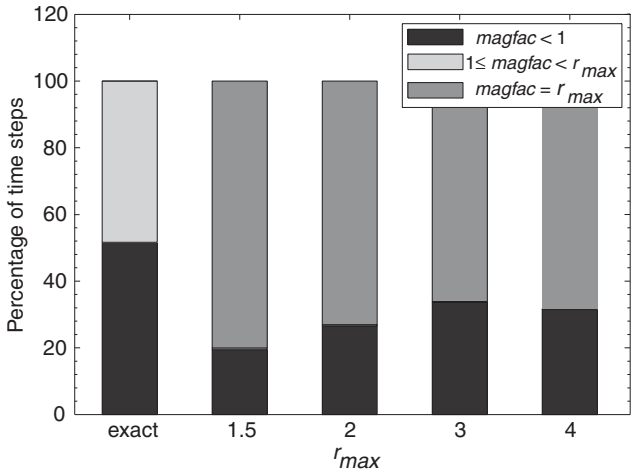

Figure 7. Classification of ATS step size magnification factor (MAGFAC) for different $r_{\max}$ values.

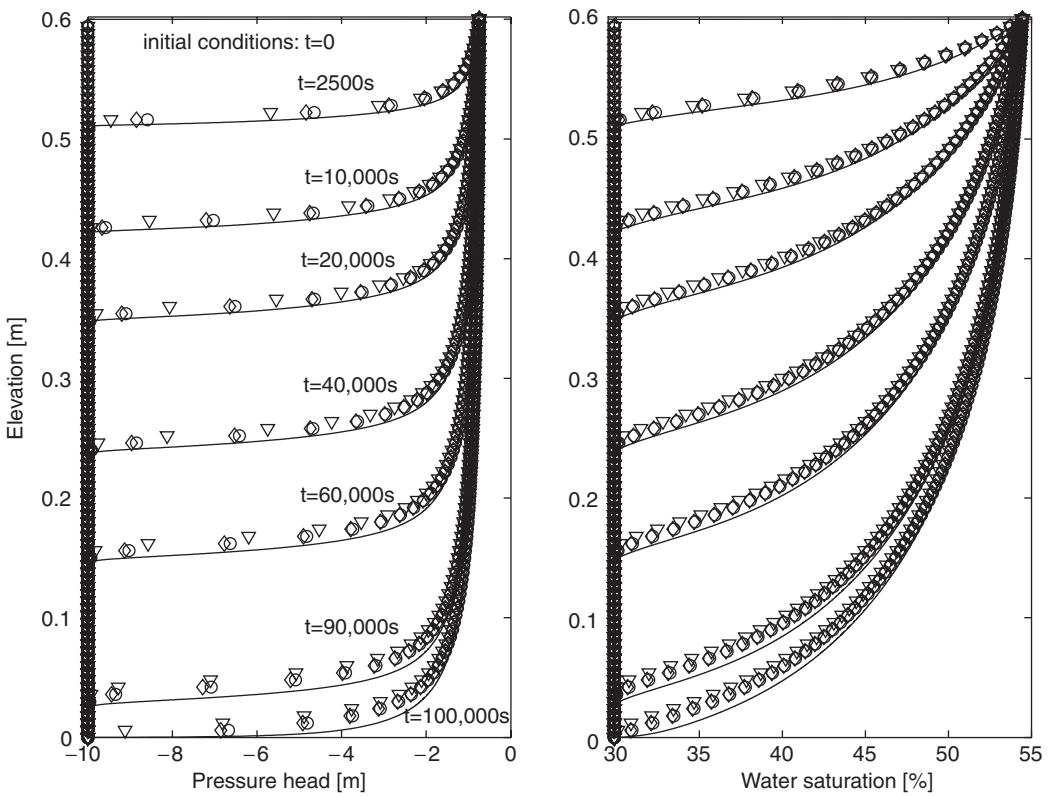

Figure 8. Pressure head and water saturation profiles for different τ_A values: 0.001 (○), 0.01 (◇), 0.1 (▽) and for the surrogate exact solution (solid line).

DOI: 10.1002/fld

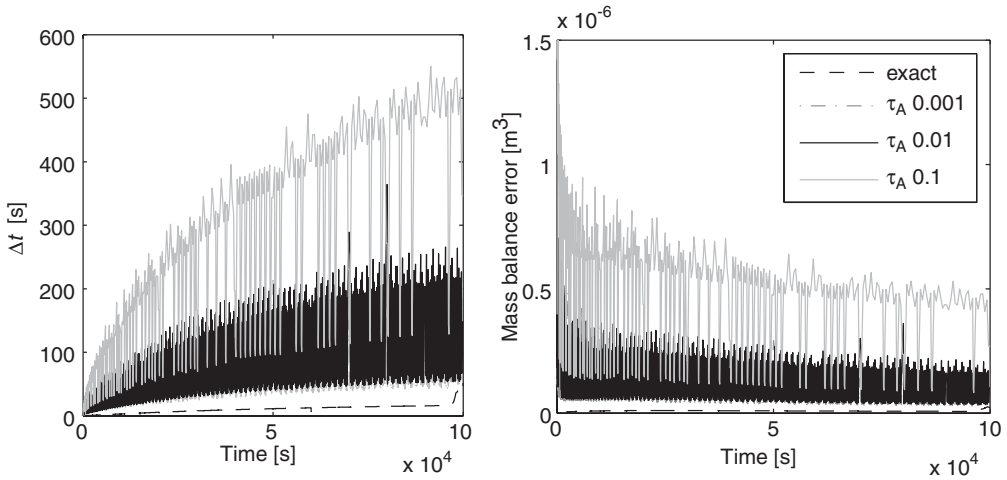

Figure 9. Evolution of Δt and mass balance error for different τ_A values.

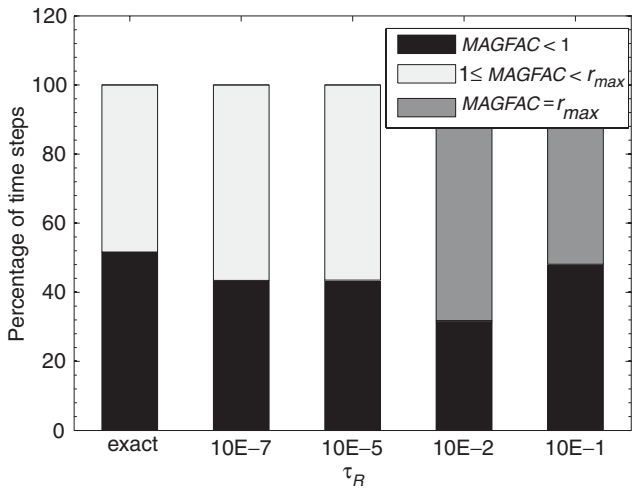

Figure 10. Classification of ATS step size magnification factor (MAGFAC) for different τ_R values.

3.2.3. Influence of τ_R. To evaluate the influence of the τ_R parameter in Equation (7), 4 simulations are compared with τ_R values of 10^{-7} ('exact' solution), 10^{-5}, 10^{-2}, and 10^{-1}. The absolute error parameter τ_A was kept constant at 0.001 and τ_{PI} was set to $0.01 \times \tau_R$.

The results are very similar to those reported for the τ_A parameter, with the lowest accuracy case ($\tau_R = 0.1$) producing an inferior solution (not shown). The ATS schemes for the $\tau_R = 10^{-5}$ and 10^{-7} runs are also very similar to the surrogate exact solution in terms of MAGFAC behaviour (Figure 10), again confirming the earlier observation concerning ATS being most effective when accuracy constraints on the solution are very rigid.

DOI: 10.1002/fld

4. CONCLUSIONS

The behaviour of different schemes for initial solution estimates and adaptive time stepping were tested for a Richards equation model. Time step adaptation is essential to achieve reasonable computing performance in realistic applications of Richards' equation. Two approaches for doing so make use of local time truncation error estimates or of the convergence behaviour of the nonlinear solver. The former approach can be considered an *a priori* technique and the latter scheme an *a posteriori* one, although there is some overlap in this classification. We also use the common but ambiguous designations 'adaptive' (ATS) and 'heuristic' (HTS) for the truncation error-based and convergence-based techniques, respectively. The various schemes were evaluated for two one-dimensional problems characterized by strongly nonlinear boundary conditions and soil hydraulic properties and sharp infiltration fronts.

For the initial solution estimates in the Picard iteration scheme used as the nonlinear solver in our model, the results show that second order extrapolation, relying on the solution at the previous three time levels, significantly improves convergence compared to the commonly used zero order estimation where only the previous time level is used. Second-order extrapolation is especially effective for the HTS time stepping approach, enabling larger and thus fewer time steps and making this approach as or more computationally efficient than the ATS method.

For the adaptive time stepping approaches, the results show that truncation error-based methods are not always to be preferred over convergence-based schemes. When simulating strong nonlinearities the size of the time step can be constrained by the convergence of the iterative scheme instead of the time truncation error. Adaptive schemes based on the latter can give rise to nonlinear solver failures that decrease the computational performance of the simulator. Although more empirical or heuristic, HTS provided a better control on the behaviour of the nonlinear iteration and resulted in more efficient simulations. Further research is needed in the development of mixed adaptive schemes that rely on both local truncation error estimation and nonlinear convergence properties. It is also observed that when accuracy constraints are low (i.e. high tolerance values), the behaviour of the ATS scheme can be dominated by its empirical parameters. This again limits to some extent the applicability of the *a priori* technique, since stringent accuracy constraints are not often used in practical simulations, in consideration of computational costs and in recognition of other sources of error (model and data) inherent in the modelling process.

ACKNOWLEDGEMENTS

We thank the two anonymous reviewers for their helpful comments.

REFERENCES

1. Gresho PM, Lee RL, Sani RL. On the time-dependent solution of the incompressible Navier–Stokes equations in two and three dimensions. *Recent Advances in Numerical Methods in Fluids*. Pineridge Press, Ltd.: Swansea, U.K., 1980; 27–80.
2. Tocci MD, Kelley C, Miller CT. Accurate and economical solution of the pressure-head form of Richards' equation by the method of lines. *Advances in Water Resources* 1997; **20**(1):1–14.
3. Diersch H-J, Perrochet P. On the primary variable switching technique for simulating unsaturated-saturated flows. *Advances in Water Resources* 1999; **23**(3):271–301.
4. Kavetski D, Binning P, Sloan SW. Adaptive time stepping and error control in a mass conservative numerical solution of the mixed form of Richards equation. *Advances in Water Resources* 2001; **24**(6):595–605.

DOI: 10.1002/fld

5. Kavetski D, Binning P, Sloan SW. Adaptive backward euler time stepping with truncation error control for numerical modelling of unsaturated fluid flow. *International Journal for Numerical Methods in Engineering* 2002; **53**(6):1301–1322.
6. Paniconi C, Putti M. A comparison of Picard and Newton iteration in the numerical solution of multidimensional variably saturated flow problems. *Water Resources Research* 1994; **30**(12):3357–3374.
7. D'Haese CMF, Putti M, Paniconi C, Verhoest NEC, De Troch FP. Assessment of initial solution estimates and adaptive vs. heuristic time stepping for variably saturated flow. In *Proceedings of the XVth International Conference on Computational Methods in Water Resources*, vol. 1. Miller CT, Farthing MW, Gray WG, Pinder GF (eds). Elsevier: Amsterdam, The Netherlands, 2004; 545–556.
8. Cooley RL. A finite difference method for unsteady flow in variably saturated porous media: application to a single pumping well. *Water Resources Research* 1971; **7**(6):1607–1625.
9. Huyakorn PS, Thomas SD, Thompson BM. Techniques for making finite elements competitive in modeling flow in variably saturated porous media. *Water Resources Research* 1984; **20**(8):1099–1115.
10. Kavetski D, Binning P, Sloan SW. Noniterative time stepping schemes with adaptive truncation error control for the solution of Richards equation. *Water Resources Research* 2002; **38**(10):1211, doi:10.1029/2001WR000720.
11. Rathfelder K, Abriola LM. Mass conservative numerical solutions of the head-based Richards equation. *Water Resources Research* 1994; **30**(9):2579–2586.
12. van Genuchten MT, Nielsen DR. On describing and predicting the hydraulic properties of unsaturated soils. *Annales Geophysicae* 1985; **3**(5):615–628.
13. Paniconi C, Aldama AA, Wood EF. Numerical evaluation of iterative and noniterative methods for the solution of the nonlinear Richards equation. *Water Resources Research* 1991; **27**(6):1147–1163.
14. Miller CT, Williams GA, Kelley C, Tocci MD. Robust solution of Richards' equation for nonuniform porous media. *Water Resources Research* 1998; **34**(10):2599–2610.
15. Vogel T, van Genuchten M, Cislerova M. Effect of the shape of the soil hydraulic functions near saturation on variably-saturated flow predictions. *Advances in Water Resources* 2001; **24**(2):133–144.
16. Williams GA, Miller CT. An evaluation of temporally adaptive transformation approaches for solving Richards' equation. *Advances in Water Resources* 1999; **22**(8):831–840.
17. Gustafsson K, Söderlind G. Control strategies for the iterative solution of nonlinear equations in ODE solvers. *SIAM Journal on Scientific Computing* 1997; **18**(1):23–39.
18. Celia MA, Bouloutas ET, Zarba RL. A general mass-conservative numerical solution for the unsaturated flow equation. *Water Resources Research* 1990; **26**(7):1483–1493.

DOI: 10.1002/fld